



*Citation for published version:*

Aggarwal, RK, Blond, SL, Beaumont, P, Baber, G, Kawano, F & Miura, S 2012, High frequency fault location method for transmission lines based on artificial neural network and genetic algorithm using current signals only. in 11th International Conference on Developments in Power Systems Protection, 2012. DPSP 2012. IET, 11th International Conference on Developments in Power Systems Protection, 2012, DPSP 2012, Birmingham, UK United Kingdom, 22/04/12. <https://doi.org/10.1049/cp.2012.0041>

*DOI:*

[10.1049/cp.2012.0041](https://doi.org/10.1049/cp.2012.0041)

*Publication date:*

2012

*Document Version*

Peer reviewed version

[Link to publication](#)

This paper is a postprint of a paper submitted to and accepted for publication in 11th International Conference on Developments in Power Systems Protection, 2012 and is subject to Institution of Engineering and Technology Copyright. The copy of record is available at IET Digital Library

## University of Bath

### General rights

Copyright and moral rights for the publications made accessible in the public portal are retained by the authors and/or other copyright owners and it is a condition of accessing publications that users recognise and abide by the legal requirements associated with these rights.

### Take down policy

If you believe that this document breaches copyright please contact us providing details, and we will remove access to the work immediately and investigate your claim.

# HIGH FREQUENCY FAULT LOCATION METHOD FOR TRANSMISSION LINES BASED ON ARTIFICIAL NEURAL NETWORK AND GENETIC ALGORITHM USING CURRENT SIGNALS ONLY

R.K. Aggarwal\*, S.L. Blond\*, P. Beaumont<sup>†</sup>, G. Baber<sup>†</sup>, F. Kawano<sup>†</sup>, S. Miura<sup>#</sup>

\*University of Bath, United kingdom, [eesrka@bath.ac.uk](mailto:eesrka@bath.ac.uk)

<sup>†</sup>Toshiba International (Europe) Ltd, United Kingdom

<sup>#</sup>Toshiba Corporation, Japan

**Keywords:** fault location, transmission lines, fault current signals, artificial neural networks, genetic algorithm.

## Abstract

The present transmission systems are rapidly changing principally due to an increasing demand for better utilisation of existing lines resulting in lower transient stability limits, and also due to an increase in the complexity of the networks with small-scale distributed generation being connected into the existing networks. The current protection/fault location techniques are not conducive to such networks. This paper investigates a novel fault location method based on current signals only and utilising Artificial Intelligence technology. Importantly, the robustness and sensitivity of the technique developed is presented through an extensive series of studies and results when applied to complex power networks.

## 1 Introduction

The present transmission systems are rapidly changing principally due to an increasing demand for better utilisation of existing lines resulting in lower transient stability limits, and also due to an increase in the complexity of the networks with small-scale distributed generation being connected into the existing networks; this in turn will have a detrimental effect on the performance of the commonly employed Distance protection (DP). Due to rapid advancements in technology, an attractive alternative to DP is the research and development of a non-unit fault locator based on transient fault-generated current signals only for both fault detection and discrimination thereby increasing both the security and dependability of protection on future, complex and rapidly changing transmission networks. Apart from its robustness, this technique has the added advantage that it obviates the need of CVTs (which have a very poor transient response), thereby resulting in considerable cost saving to the Electricity Supply Industry worldwide.

Fault generated transients in EHV transmission lines caused by a sudden change in system voltage due, for example, arcing faults, are generally either severely attenuated or are outside the bandwidth of most conventional fault location schemes using traditional transducers. They are treated as noise and extensive research has been conducted to accurately extract the power frequency component and much useful information within the fault transients is lost. In [1,2], fault generated high frequency components are used to develop new relay principles which could solve the problems mentioned above. Although these schemes can offer the complete protection of a transmission line, they employ conventional power line communication signal traps at both ends of the protected line, which are costly and importantly, are found only in a limited number of EHV transmission systems.

In [3], the author presents a new non-communication protection scheme for discriminating internal and external faults for a whole variety of different system and fault conditions and make use of the fault generated high frequency current signals. Although the results presented demonstrate a high performance, the technique developed is heavily dependent on an accurate design of multi-channel digital filters (this adds significantly to the complexity of the protection technique). In [4], the authors have introduced an approach based on Wavelet Transform and Artificial neural network (ANN) to classify internal and external faults using voltage signals. However, due to the CVT bandwidth limitation, the high frequencies associated with the voltage need to be obtained by additional devices such as specially designed high frequency voltage detectors. The relays designed based only on current transients are more practical and well suited in making use of high frequency in current signals by virtue of the wide bandwidth (>70 kHz) of CTs.

The technique presented herein involves extracting the transient signal components from the fault-generated current signals via a high-pass filter (500Hz and above), which are non-stationary in nature; this high-pass filter has been chosen principally by virtue of the fact that through an extensive

series of studies, it was found that the features in the transient signals varied with fault location. The Artificial Intelligence fault location technique described in this paper is based on the information above 500 Hz. Below 500 Hz, the power frequency component was found to be too dominant and tended to swamp the secondary features that depended on fault distance. The high pass filter is thus kept at a constant cut off frequency of 500 Hz.

The key to the development of the novel fault location algorithm is the feature selection and the optimal architecture of the ANN. In this respect, the former is based on the spectral energy of the transient signal components occurring specifically at certain peaks in the frequency spectra; these then form the basis of training ANNs, the architectures of which are optimised using the genetic algorithm (GA) approach. GA; this is a global search and optimisation technique based on the driving mechanism behind evolution and is particularly well suited for the optimisation of the ANN architecture which by nature, represents a multi-dimensional problem.

The performance and robustness of the fault location algorithm is illustrated by applying it to a typical 400 kV UK transmission network, in particular, under i) different types of fault; ii) fault resistance and iii) source capacity variations.

## 2 Outline of methodology

This section outlines a summary of the methodology developed essentially to facilitate/appreciate the various case studies (and the associated results attained) so as to assess the performance of the developed fault location algorithm, under a variety of different fault types, variation in both fault resistance and source capacities.

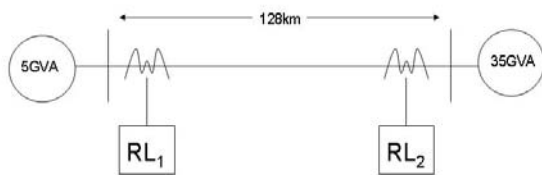


Figure 1: The system configuration studied

ATP-EMTP is used to give a series of time domain waveforms for various faults at different distances in the system configuration shown in Fig 1. The sampling frequency of the simulation was 100 kHz and the simulation was run for 20ms (1 cycle at 50 Hz).

Transient current waveforms are then imported into MATLAB. The Fast Fourier Transform (FFT) is used to transform the signals into the frequency domain. Information below 500 Hz is filtered out to eliminate the dominant power frequency component in the signal.

### 2.1 Feature selection

Each spectrum has a distinctive maximum peak. Fig 2 typifies one such peak and demonstrates how the peak varies on the faulted phase. The location of this peak varies with fault location, but crucially *does not* vary with fault inception point on the waveform. Only the magnitude of this peak varies with inception point. This means that regardless of where the fault occurs on the waveform, the peak feature will always be in exactly the same place.

In [5], this peak is referred to as one of the ‘natural’ frequencies. These are the modes of oscillation that arise on the transmission line due to the travelling waves being reflected back and forth from the fault origin and the terminating buses, due to the discontinuities at these locations. The variation of the peak with fault distance in [5] shows good agreement with simulation results attained.

Figs 3 and 4 show how the location of the maximum peak varies with fault distance, for the healthy and faulted phases, respectively. The scales are normalised between 1 and 0.

The drawback of the minimum inception point is that the magnitude of the first peak is often lower than the exponentially decaying background frequency spectra. This introduces difficulty in determining the location of the maximum peak.

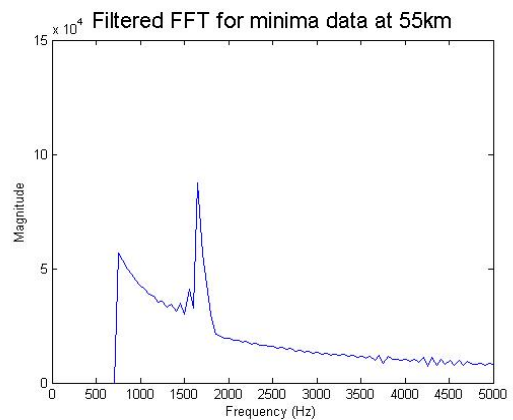


Figure 2: Fault at 55 km, the maximum peak occurring at 1650Hz

### 2.2 Additional Feature

As mentioned previously, the location of the peak at some fault distances is unreliable. To address this, an additional feature was added to the feature selection stage. In this case, this is simply the area under the frequency spectrum. This was shown to vary with fault location in Fig 5 for the faulted phase.

### 2.3 Artificial Neural Networks (ANNs)

Fig 6 shows an overview of the proposed method. In the feature selection stage the raw current spectra are evaluated to

determine the location of maxima peak and the amount of spectral energy for each phase. These form the six inputs to

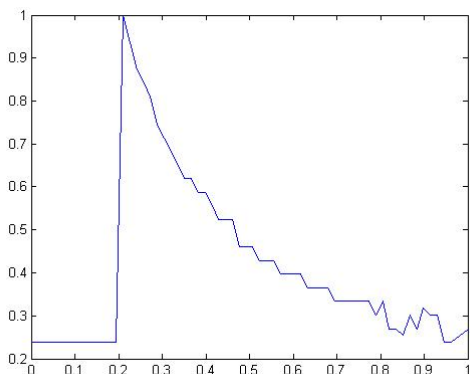


Figure 3: The normalised variation of location of peak on the faulted phase distance

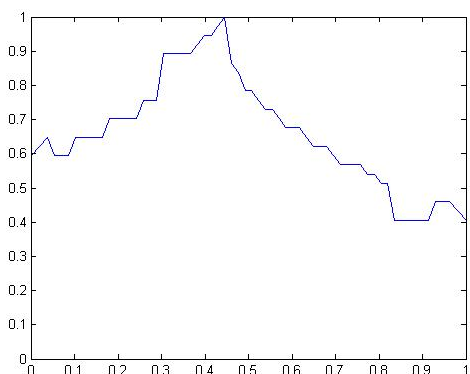


Figure 4: The variation of location of peak with distance on the healthy phases

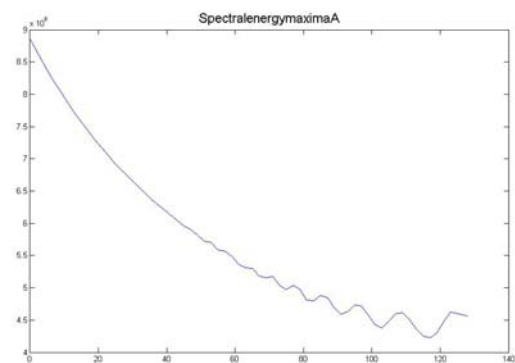


Figure 5: The faulted phase's spectral energy variation with distance, for a maxima inception point.

an ANN, which is described in section 2.5. The output neuron gives the fault location as a percentage of the line length.

## 2.4 Genetic Algorithms

The optimization of the ANN architectures represents a multidimensional search problem. A well suited technique for this is the genetic algorithm (GA). The genetic algorithm is a

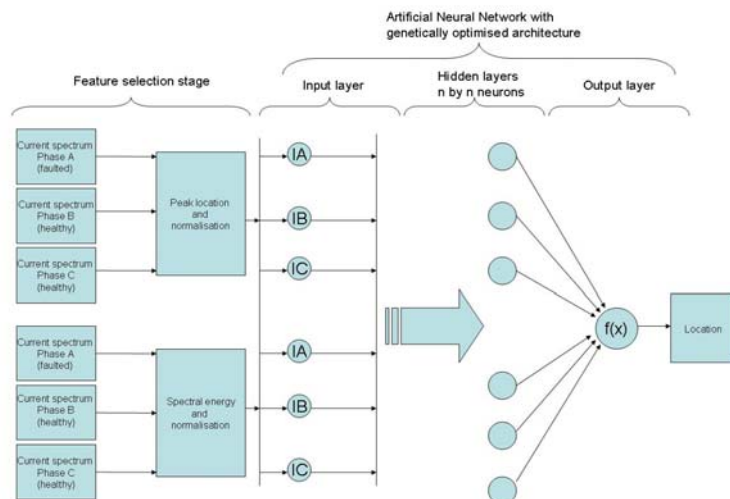


Figure 6: Flow diagram of developed method

global search and optimization technique based on the driving mechanisms behind evolution, such as natural selection and mutation in the reproductive process. Fig 7 illustrates a basic overview of the genetic algorithm.

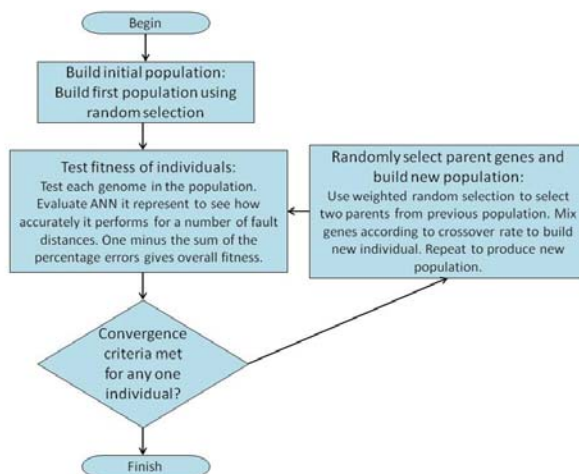


Figure 7: A basic overview of the genetic algorithm

## 2.5 Optimisation of architecture

As discussed earlier, there are a large number of parameters involved in the design of an ANN. Obviously a network that is too small and simple will not be able to discern non-linearity between inputs and outputs. However a network that is too large (i.e. has too many hidden layers or neurons in each layer) will take longer to evaluate. Moreover, overly large networks are known not to perform well in the presence of unknown data, i.e. it loses its ability to generalise. The usual approach is to begin with a large network, and prune the architecture heuristically, removing neurons until the network performance begins to suffer. This is the approach to ANN fault location developed in [6]. However, in [6], the inputs are voltage and current magnitudes based at power frequency.

The GA is thus applied herein in optimizing the ANN parameters to give the best performing network for the task. This formalises and greatly speeds the process of building the network.

### 3 Results and discussion

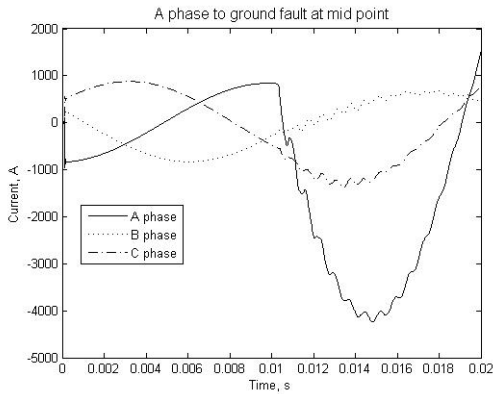


Figure 8: Current waveforms for an A-phase-earth fault

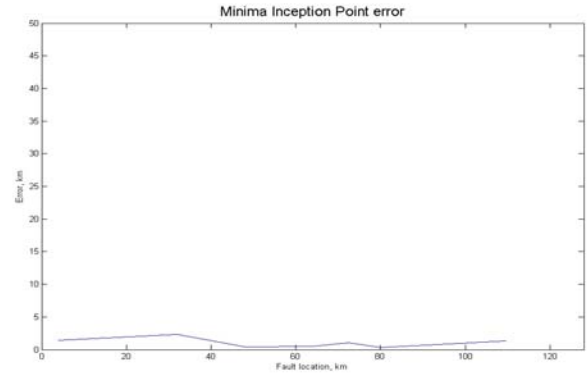
Fig 8 illustrates typical fault current waveforms for an A-phase-earth fault at the midpoint of the line.

Fig 9 typifies the performance of the developed technique for single-phase-earth faults on the system shown in Fig 1. It is clearly evident that the algorithm developed displays a high degree of accuracy in fault location for faults at all points on the line (both for maximum and minimum fault inception angles), the maximum error being <2%.

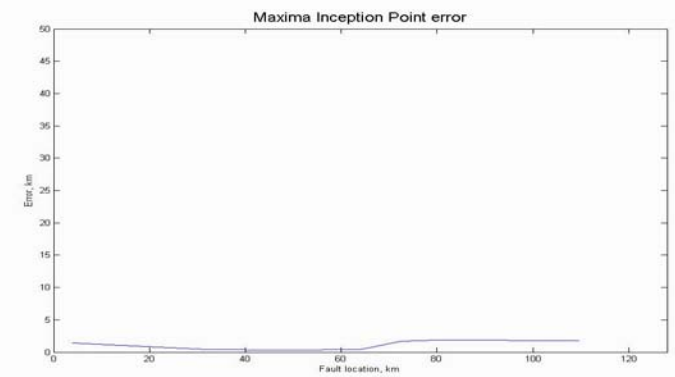
The rest of the results presented herein are essentially to ascertain the robustness and the sensitivity of the previously developed algorithm (genetically optimised trained ANN for the single-phase-to-earth fault only) which is tested for different types of fault, variable fault resistance and a variation in source capacities.

#### 3.1 Effect of different types of fault

Phase-to-phase-earth faults were simulated at five test locations: 4, 32, 64, 96, 123 km on the system configuration shown in Fig 1. The actual fault location was compared to the fault location predicted by the ANN.



9 (a)

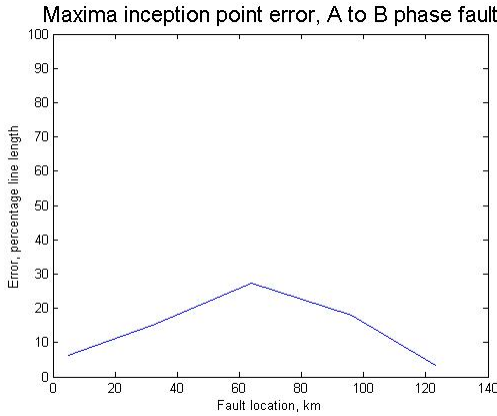


9 (b)

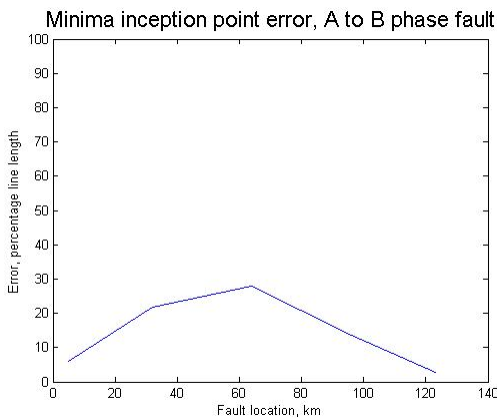
Figure 9: Fault location error for a single-phase – earth fault (a) Voltage minimum fault (b) Voltage maximum fault

- i) Fig 10 (a) shows the Algorithm response for a phase to phase fault when the inception point is at the maximum on the A-phase for an A-to-B-phase fault.
- ii) Likewise, Fig 10 (b) shows the Algorithm response for a phase to phase fault when the inception point is at the minimum on the A-phase for an A-to-B-phase fault.

Bearing in mind good performance is signified by a horizontal straight line close to the X-axis, Fig 10 shows the ANN performs rather poorly for both the maxima and minima inception cases for a phase to phase fault. This is somewhat expected since the features at the feature selection stage are very different for the B-phase on an A-to-B-phase fault compared to an A-phase-to-earth fault. Thus both the spectral energy and the maximum peak will be considerably different for this phase. This is also the case for a phase-to-phase-earth fault.



10 (a)



10 (b)

Figure 10: Response for A-to-B-phase fault at  
(a) Fault at  $V_{AB \max}$   
(b) Fault at  $V_{AB \min}$

### 3.2 Effect of fault resistance

A-phase-earth faults were simulated at five test locations: 5, 32, 64, 96, 123 km. The actual fault location was compared to the fault location predicted by the ANN. As can be clearly seen from Fig 11, the algorithm again performs poorly for faults of a varying resistance, especially for faults close to the relay. Just for comparison, Fig 11 also shows the response for a fault resistance of 2  $\Omega$  which was the fault resistance employed in the development of the original algorithm. As can be seen, there is a significant deterioration in the performance in case of a 25  $\Omega$  fault resistance. This can be attributed to several likely reasons.

Following a fault, the relay sees the impedance of the line, together with the impedance of the fault, which in this case is purely resistive. When the fault is close in, the fault resistance has much more effect as it constitutes a higher proportion of the resistance in the current path. Thus the variation between the trained case at 2  $\Omega$  and the test case is greater. It is already difficult to discern the location of the peak for close up faults since the 50 Hz lobe tends to dominate this area of the spectrum, and the varying resistance compounds this issue. The secondary feature, (being the area under the spectrum), is

also much different since the greater the resistance, the less current that flows to ground and so the lower the magnitude at every frequency.

### 3.3 Effect of source capacity

Here, the source capacities were varied from the original 5 GVA and 35 GVA at the two ends (Fig 1), to 35 GVA and 35 GVA.

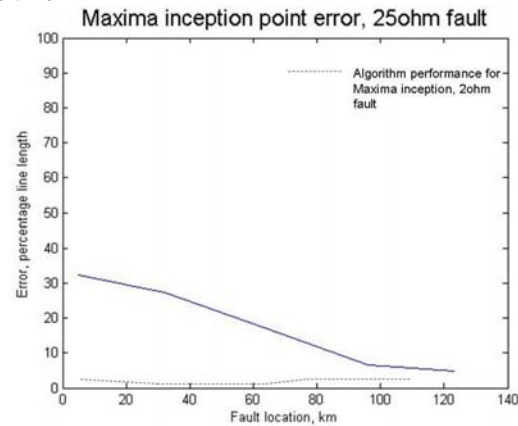


Figure 11: Response for fault resistance of 25 ohms

Phase-to-phase-earth faults were simulated at five test locations: 5, 32, 64, 96, 123 km, and for comparative purposes, faults for A-phase-earth faults were also simulated for the same fault locations. The actual fault location was compared to the fault location predicted by the ANN. From Fig 12, it is apparent that when the source capacities are varied significantly, the ANN does not perform particularly well for this system condition for the phase-to-phase-earth fault considered. However, this is in marked contrast to the results for the single-phase-earth fault (Fig 13) which shows a high performance in the accuracy of fault location (overall error <2%). In the case of the former, because like the case for a change in fault resistance, a change in source capacity (concomitant with a different fault type), causes the input data to change in a statistically significant way, and this variation has not been accounted for in the training data.

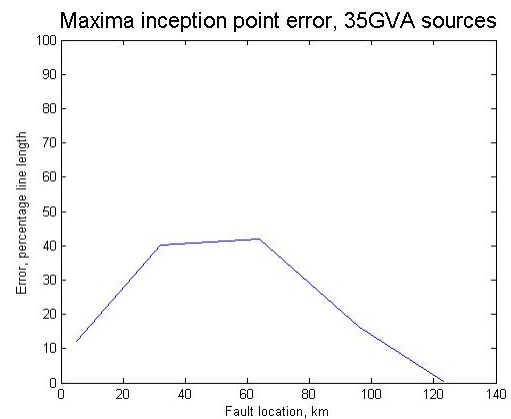


Figure 12: Response for phase-to-phase-earth fault for source capacities of 35 GVA and 35 GVA

The ANN has not been trained with other types of fault, higher resistance cases or alternative source capacities.

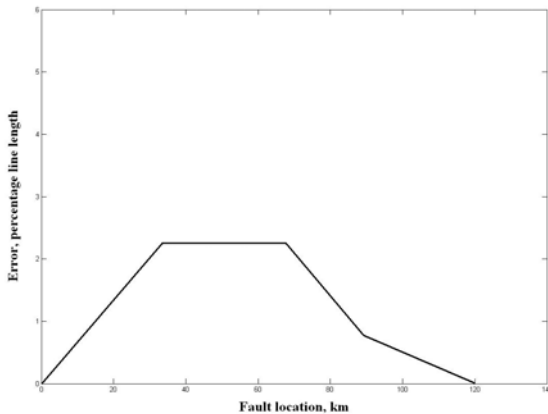


Figure 13: Response for single-phase-earth fault for source capacities of 35 GVA and 35 GVA

## 4 Conclusions

The results presented herein clearly demonstrate that the originally trained ANN (which was trained for only single-phase-earth faults with a fault resistance of 2  $\Omega$  and source capacities of 5 GVA and 35 GVA at the two ends), whilst giving a high performance in fault location accuracy for single-phase-earth faults, performs rather poorly when subjected to data for other types of fault, a large variation in both fault resistance and source capacities. This would be expected by virtue of the fact that once trained, the ANN sets up a feature space (based on the original training data) and any significant digression in a change in patterns arising for example, due to different fault types, significant variation in fault resistance and source capacity, would be well outside the feature space of the ANN. However, it must be mentioned that the trained ANN is quite robust to small levels of non-algorithmic errors of within  $\pm 5\%$ , arising for example, due to a variation in line length, fault resistance, source capacity, etc. The overall error in fault location (in particular for phase-earth faults), will still remain  $< \pm 2\%$ .

### 4.1 Solution to the problem (as part of future work)

One of the most effective ways of overcoming the aforementioned problem would be to adopt a modular approach whereby there will be a subset of the overall fault location methodology comprising of a number of trained ANNs, one for each type of fault viz, phase-earth, phase-to-phase, two-phase-earth and three-phase-earth. By including fault cases involving different levels of fault resistance (low to high) and different source capacities for each of the ANNs, as part of the training data, the performance of the overall fault location technique would be significantly improved (likely to be  $< \pm 5\%$  error). A modular approach would also provide the flexibility to deal with other important degrees of freedom. In this respect, it should be mentioned that training one single ANN to cater for all conceivable scenarios would

introduce prohibitive complexity in the calibration and commissioning of a commercial device.

It should be noted that although a modular approach can be lengthy and time consuming, the optimised weights for each ANN require relatively little memory within the hardware and once a particular type of fault has been identified, the appropriate ANN can be activated. The technique for identifying fault type/phase selection is well developed and is relatively simple to implement. Importantly, it should also be mentioned that the developed methodology as presented herein for the optimisation of the features using GAs for training the ANN, can equally well be applied to the sub-set of ANNs without requiring any additional modifications.

Finally, an important step in the validation of this approach would be a software program that was able to iterate through a number of ATP fault scenarios, as this is the most labour intensive part of the process. With this facility, an arbitrarily large bank of fault cases could be quickly established and it would be possible to use a selection of these to train a genetically optimised ANN with a separate MATLAB macro. It could also be relatively quickly established how feasible the approach was for commercial development.

## 5 Acknowledgements

The authors (particularly from Bath) are grateful to Toshiba International (Europe) Ltd for providing the funding for the project on which this paper is based on.

## 6 References

- [1] A. T. Johns, R. K. Aggarwal, and Z. Q. Bo, "Non-unit protection technique for EHV transmission systems based on fault-generated noise. Part 1: signal measurement", *Generation, Transmission and Distribution*, IEE Proceedings-, vol. 141, pp. 133-140, 1994.
- [2] R. K. Aggarwal, A. T. Johns, and Z. Q. Bo, "Non-unit protection technique for EHV transmission systems based on fault-generated noise. Part 2: signal processing", *Generation, Transmission and Distribution*, IEE Proceedings-, vol. 141, pp. 141-147, 1994.
- [3] Z. Q. Bo, "A new non-communication protection technique for transmission lines", *Power Delivery*, IEEE Transactions on, vol. 13, pp. 1073-1078, 1998.
- [4] Z. Nan and M. Kezunovic, "Transmission Line Boundary Protection Using Wavelet Transform and Neural Network", *Power Delivery*, IEEE Transactions on, vol. 22, pp. 859-869, 2007.
- [5] X.G. Wang, et al, "Study of transient spectrum in transmission lines", *IEEE PES meeting- Conversion of delivery of Electrical Energy in the 21<sup>st</sup> century*, IEEE PES 2008
- [6] T. Bouthiba, "Fault location in EHV transmission lines using artificial neural networks", *Int. Journal of Appl. Maths, Computer Science*, vol.14, pp 69-78.